

Durham Research Online

Deposited in DRO:

15 March 2016

Version of attached file:

Published Version

Peer-review status of attached file:

Peer-reviewed

Citation for published item:

Rasmussen, C. M. Ø. and Ullmann, C. V. and Jakobsen, K. G. and Lindskog, A. and Hansen, J. and Hansen, T. and Eriksson, M. E. and Dronov, A. and Frei, R. and Korte, C. and Nielsen, A. T. and Harper, D. A. T. (2016) 'Onset of main Phanerozoic marine radiation sparked by emerging Mid Ordovician icehouse.', *Scientific reports.*, 6 . p. 18884.

Further information on publisher's website:

<http://dx.doi.org/10.1038/srep18884>

Publisher's copyright statement:

This work is licensed under a Creative Commons Attribution 4.0 International License. The images or other third party material in this article are included in the article's Creative Commons license, unless indicated otherwise in the credit line; if the material is not included under the Creative Commons license, users will need to obtain permission from the license holder to reproduce the material. To view a copy of this license, visit <http://creativecommons.org/licenses/by/4.0/>

Use policy

The full-text may be used and/or reproduced, and given to third parties in any format or medium, without prior permission or charge, for personal research or study, educational, or not-for-profit purposes provided that:

- a full bibliographic reference is made to the original source
- a [link](#) is made to the metadata record in DRO
- the full-text is not changed in any way

The full-text must not be sold in any format or medium without the formal permission of the copyright holders.

Please consult the [full DRO policy](#) for further details.

SCIENTIFIC REPORTS

OPEN

Onset of main Phanerozoic marine radiation sparked by emerging Mid Ordovician icehouse

Received: 28 September 2015

Accepted: 30 November 2015

Published: 06 January 2016

Christian M. Ø. Rasmussen^{1,2,3}, Clemens V. Ullmann^{4,5}, Kristian G. Jakobsen⁶, Anders Lindskog², Jesper Hansen⁷, Thomas Hansen⁷, Mats E. Eriksson², Andrei Dronov⁸, Robert Frei^{4,9}, Christoph Korte⁴, Arne T. Nielsen¹ & David A.T. Harper¹⁰

The Great Ordovician Biodiversification Event (GOBE) was the most rapid and sustained increase in marine Phanerozoic biodiversity. What generated this biotic response across Palaeozoic seascapes is a matter of debate; several intrinsic and extrinsic drivers have been suggested. One is Ordovician climate, which in recent years has undergone a paradigm shift from a text-book example of an extended greenhouse to an interval with transient cooling intervals – at least during the Late Ordovician. Here, we show the first unambiguous evidence for a sudden Mid Ordovician icehouse, comparable in magnitude to the Quaternary glaciations. We further demonstrate the initiation of this icehouse to coincide with the onset of the GOBE. This finding is based on both abiotic and biotic proxies obtained from the most comprehensive geochemical and palaeobiological dataset yet collected through this interval. We argue that the icehouse conditions increased latitudinal and bathymetrical temperature and oxygen gradients initiating an Early Palaeozoic Great Ocean Conveyor Belt. This fuelled the GOBE, as upwelling zones created new ecospace for the primary producers. A subsequent rise in $\delta^{13}\text{C}$ ratios known as the Middle Darriwilian Isotopic Carbon Excursion (MDICE) may reflect a global response to increased bioproductivity encouraged by the onset of the GOBE.

The classic studies of Sepkoski^{1,2} on Phanerozoic biodiversity change indicated a major increase in biodiversity during the Mid Ordovician – a conclusion supported by the development of more recent databases and sophisticated investigative tools although the inferred amplitude of the diversity spike varies^{3–5}. All studies strongly indicate a prolonged Early Palaeozoic radiation that markedly changed the composition and structure of Phanerozoic seascapes (Fig. 1).

The main radiation of the GOBE is generally agreed to have occurred during the Mid Ordovician Darriwilian Stage^{6,7}. Both dominant benthic and planktonic fossil groups show the same diversity pattern^{8,9}. These often display a two-phased rise in diversity with an onset in the late Floian–early Dapingian and a second main spike during the mid Darriwilian. These marked peaks consolidated a more gradual rise in species richness within some groups, notably the phytoplankton, which was initiated during the late Cambrian¹⁰.

What caused the GOBE has been intensively debated^{6,11–15}. Suggested drivers include both intrinsic and extrinsic factors, including increased complexity in the food web, a cooling climate perhaps driven by continental arc collisions, and even an extra-terrestrial spur to life. A number of these studies suggested a link with global cooling although palaeoclimatic data supporting cooler climate during the onset of the GOBE have been lacking; these data were either model driven with limited ground truthing or they have been questioned due to potentially flawed analytical techniques¹⁶. Here, we demonstrate that there is a remarkable coherence between abiotic and biotic

¹Natural History Museum of Denmark, University of Copenhagen, Øster Voldgade 5-7, 1350 Copenhagen K, Denmark. ²Department of Geology, Lund University, Sölvegatan 12, S-223 62 Lund, Sweden. ³Center for Macroecology, Evolution and Climate, University of Copenhagen. ⁴Department of Geosciences and Natural Resource Management, University of Copenhagen, Øster Voldgade 10, 1350 Copenhagen K, Denmark. ⁵Camborne School of Mines, College of Engineering, Mathematics and Physical Sciences, University of Exeter, Penryn Campus, Penryn, Cornwall TR10 9FE, U.K. ⁶Ministry of Mineral Resources, Maneq 1A, 201, P.O. Box 930, 3900 Nuuk, Greenland. ⁷Akvaplan-Niva, High North Research Centre 9296 Tromsø, Norway. ⁸Geological Institute of the Russian Academy of Sciences, Moscow, Russian Federation. ⁹Nordic Center for Earth Evolution (NordCEE), University of Copenhagen. ¹⁰Palaeoecosystems Group, Department of Earth Sciences, Durham University, Durham DH1 3LE, UK. Correspondence and requests for materials should be addressed to C.M.Ø.R. (email: christian@snm.ku.dk)

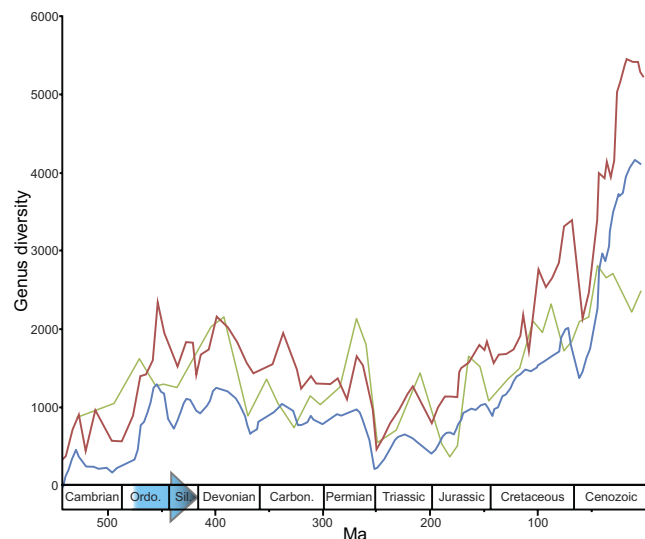


Figure 1. Estimates of Phanerozoic marine generic biodiversity. Red line based on Sepkoski²; blue line based on Rohde and Muller⁵ and green line based on Alroy *et al.*⁴. Note that the green line is not to scale (maximum number of genera approximately 500). Blue arrow indicates the main onset of the GOBE^{2,5,8,9}, including its possible prolonged duration into the Silurian Period⁴. Sepkoski's dataset downloaded from <http://strata.geology.wisc.edu/jack/>.

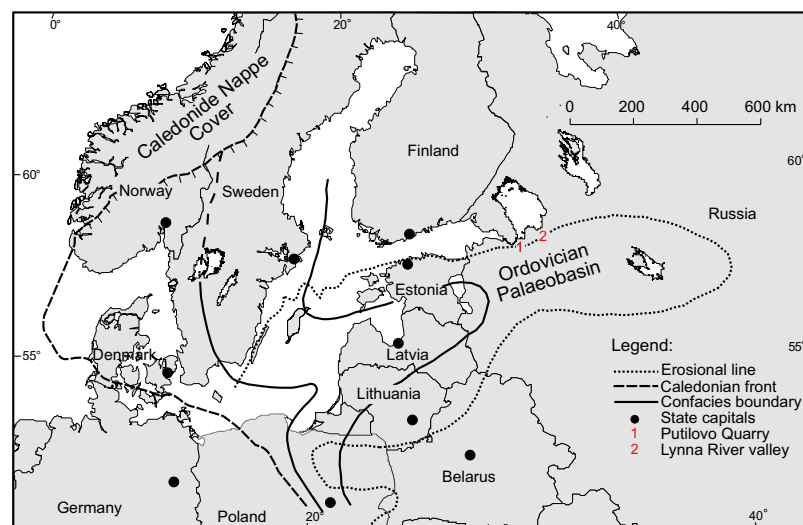


Figure 2. Facies belts of Baltica during the Mid Ordovician with location of study sites indicated. 1, Putilovo Quarry; 2, Lynna River valley. See legend for explanation of main geographical and geological features. Facies belts are shallowing towards the East. The map is modified from Hints & Harper (2003)⁵⁶ with permission.

proxies – almost bed-by-bed – which show clear evidence that a cooling indeed took place and that the GOBE seems to track this temperature decrease.

Geological setting and location of study area

The Ordovician Period was characterized by a rapid, northward drift of several palaeoplates that had rifted off Gondwana¹⁷. This intense plate tectonic activity resulted in an extreme first-order sea level rise that potentially culminated in a Phanerozoic sea level maximum in the Late Ordovician^{18,19} generating widespread epicontinental seas which have no modern analogues. One of these extensive seas was established across large parts of the palaeocontinent of Baltica (Fig. 2). During the Early–Mid Ordovician, Baltica moved rapidly from the cool temperate climate zone at about 50°S towards warmer temperate latitudes, reaching about 40°S in the mid Darriwilian¹⁷. Thus, the more shallow-water facies of this palaeobasin is characterized by cool-water carbonates²⁰. Overall, the depositional facies changed westwards in Baltoscandia from nearshore, detritic wacke–grainstones intercalated

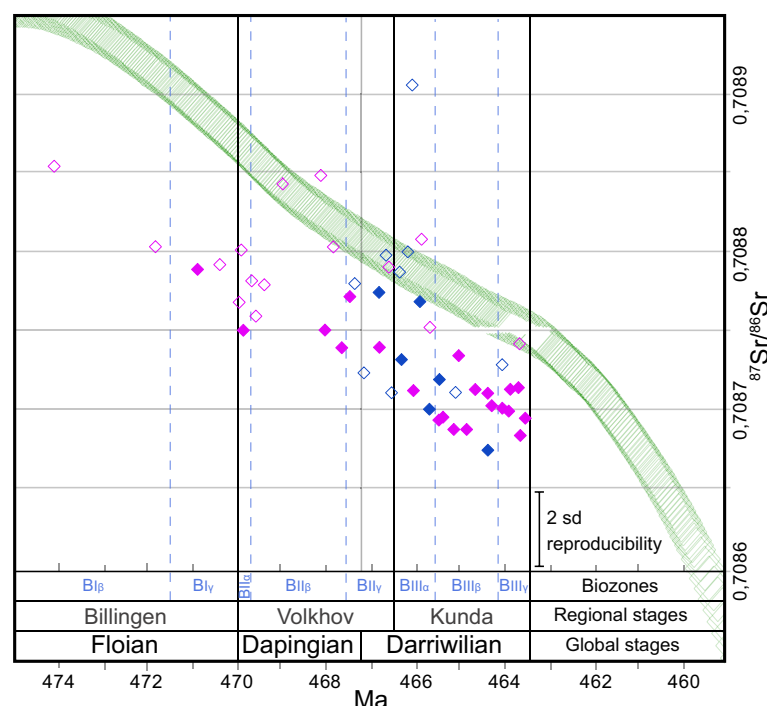


Figure 3. $^{87}\text{Sr}/^{86}\text{Sr}$ Strontium ratios plotted against stratigraphy based on 51 brachiopod specimens from the two studied sections. Inferred global trend based on the LOWESS fitted line²³ (marked in green) is included for comparison. Solid pink rhombs indicate Putilovo Quarry; blue, Lynna River valley. Open rhombs represent samples with trace element composition above the operational preservation limit applied. Thus, these are regarded as less trustworthy. Error bar on the reference material is shown in the lower right corner. See Supplementary Information file for details of uncertainties in the analyses.

with marls, through finer grained limestones without marl interbeds to offshore graptolitic shales in the deepest parts of the palaeobasin. Overall, siliciclastic input was extremely limited.

The upper Lower to Middle Ordovician (Floian–Darriwilian) succession was intensively sampled bed-by-bed during several field campaigns in the St. Petersburg area, Russia and northern Estonia. The main outcome has been a very large palaeobiological dataset that precisely pinpoints the initiation of the GOBE based on a study of more than 30,000 rhynchonelliformean brachiopods²¹. Together with 15,000 trilobites, this dataset provides an exceptionally detailed mid-latitude palaeoecological window into the biotic changes on the palaeocontinent of Baltica at this time. In addition, we compiled a geochemical dataset with stable isotope and trace element data for each bed in the succession, based on more than 200 brachiopod shells.

The setting on the interior of a large stable craton provides an ideal laboratory for the study of sea level changes during the Ordovician, as local depth was little affected by tectonic disturbances. The entire Ordovician succession is condensed with a total thickness of less than 100 m in the study area. Net depositional rates were extremely low with average sedimentation rates of less than 2 mm per 1000 years and thus the effect on local water depth and, with that, on seawater temperature was minor. Furthermore, the craton was deeply peneplaned and characterized by an exceptionally low relief²⁰. In this type of depositional setting even small fluctuations in the eustatic sea level predisposed vast areas to either exposure or flooding. At the same time, the basin had a wide, ocean-facing gateway encouraging the circulation of water across the craton. This is confirmed by the fauna representing fully marine conditions supporting euhaline conditions. In addition, due to limited burial, the region has been little affected by subsequent diagenesis which is corroborated by pristine fossil preservation as displayed by elemental distribution and the well-preserved ultrastructure of the analyzed brachiopod shells (Supplementary Information and Supplementary Figs 1–3).

We focused on two sections, Putilovo Quarry and the Lynna River valley, which are located 80 km apart in western Russia (Fig. 2; Supp. Figs 1 and 2). The sections are correlated using macrofossils and fluctuations in the geochemical signals are also easily tracked in the respective sections. Global correlations of the sections are further confirmed by excursions in $\delta^{13}\text{C}_{\text{carb}}$ ²² and $^{87}\text{Sr}/^{86}\text{Sr}$ chemostratigraphy – the latter matching the declining Floian–Mid Darriwilian secular trend of the fitted LOWESS line²³ (Fig. 3).

Bed-by-bed correlation of sections

The Lower-Middle Ordovician succession in Baltoscandia is divided into trilobite zones that can be correlated across the entire region. The trilobite zones have been assigned regional index numbers which are used across the eastern part of the Baltoscandian craton. The index numbers are used in the figures herein along with the regional stages, as they allow for high precision correlation of sections. We have further tied them to global stages using

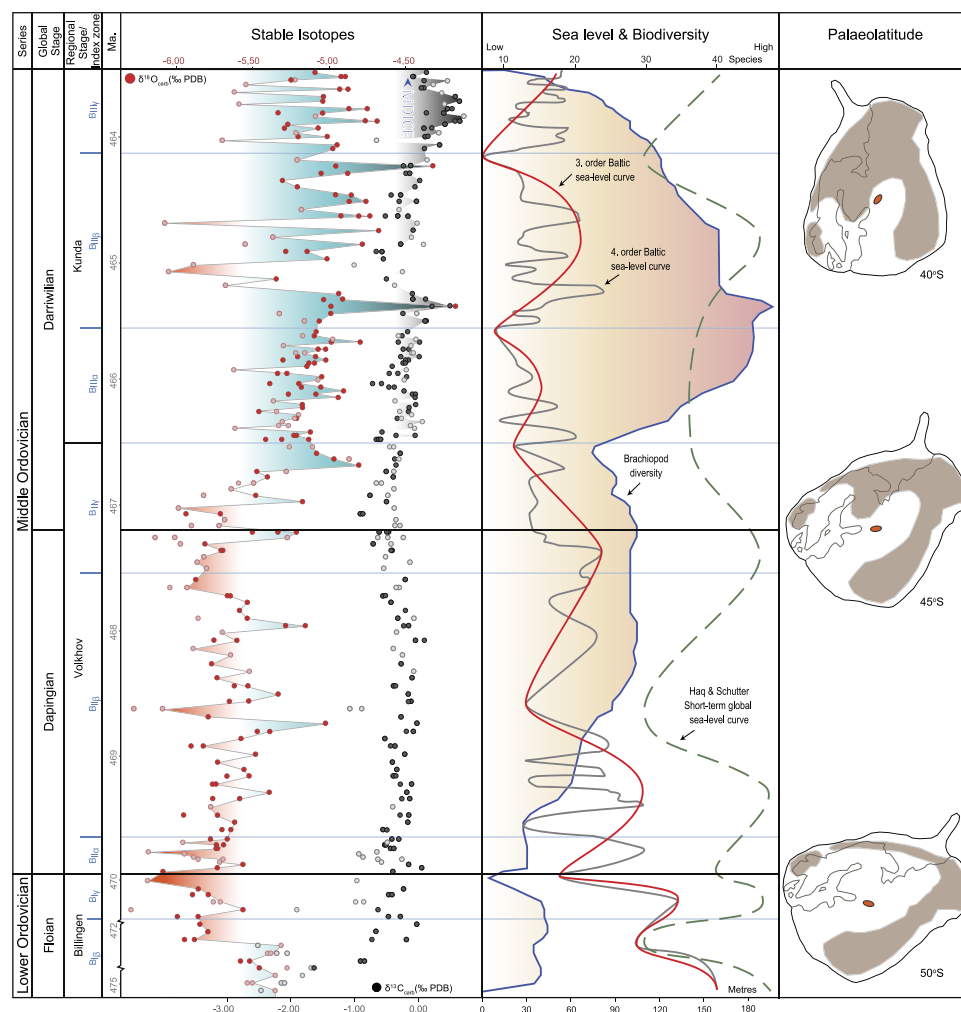


Figure 4. Summary figure showing bed-by-bed stable isotope geochemistry, sea level change and rhynchonelliform brachiopod diversity²¹ through the studied interval. In addition, the palaeogeographical northward move and anti-clockwise rotation of Baltica¹⁷ is illustrated along with our tentative approximation of Baltoscandian land areas through the studied interval (brown shading) and the location of the study area (red oval). Solid circles in the stable isotope column denote samples below the operational preservational limit; open circles are samples above. Onset of MDICE-excursion indicated in the $\delta^{13}\text{C}_{\text{carb}}$ curve. Green, punctuated line shows global, short-term fluctuations¹⁸. Abbreviations: Ma, million years.

conodont and graptolite biostratigraphy²⁴. See Supplementary Figs 1 and 2 for a schematic overview of the trilobite zones, index numbers, regional and global stages used in the current study. In Figs 3 and 4 they are further linked to chronostratigraphical ages using the most recent time scale²⁵. $^{87}\text{Sr}/^{86}\text{Sr}$ ratios, analyzed specifically on 51 brachiopod shells for the current study, corroborate these age estimates. They provide the first cluster of $^{87}\text{Sr}/^{86}\text{Sr}$ ratios from the Ordovician of Baltica and thus further refine the global data through an interval that previously had little data coverage²³. This is arguably why our data points plot a little lower than the inferred global trend represented by the LOWESS fitted line²³ (Fig. 3).

In the East Baltic area, the horizontally stratified limestone succession is condensed. Thus, the approximately 16 m of section in the Putilovo Quarry, which form the basis for the current study, correspond to a 10–12 myr interval ranging from the Lower Ordovician Floian (Fl1, *Prioniodus elegans* conodont Zone) to the Middle Ordovician Darriwilian (Dw2, *Eoplacognathus pseudoplanus* conodont Zone)²². In Putilovo Quarry roughly 150 beds were sampled, whereas in the less condensed Lynna River valley section, which encompasses the Dapingian (Dp3) – Darriwilian (Dw2) interval, approximately 100 beds were sampled. High precision correlation was achieved by using brachiopods and trilobites, which enabled a bed by bed biostratigraphical correlation^{21,26–31}. The biostratigraphical correlations were further refined by establishing biofacies which facilitated correlation within an ecostratigraphical framework^{26,31}. Thus correlation of these sections is exceptionally well constrained.

Although the two studied sections are part of the same facies belt, they represent an oblique depth transect into the eastern part of the basin: The Putilovo section is more proximal which is most evident in the lower part of the Kunda Regional Stage (Dw2), which thins westwards from more than 3 m in the Lynna River valley section

to roughly 0.5 m in the Putilovo section. This interval marks the start of the main biodiversity pulse within the shelly benthos^{21,26}.

Establishing statistically supported biofacies: the basis for the sea level curve. In order to construct a high resolution sea level curve through the sections, statistically supported biofacies were established bed-by-bed based on more than 45,000 macrofossils^{26,31}. The data were analyzed using detrended correspondence analyses and cluster analysis in the software package PAST³². The precise multivariate methods applied are described in the literature^{26,33}.

The multivariate data analyses support the establishment of a set of trilobite and brachiopod biofacies. This study operates with five depth-related biofacies of which the shallowest is based exclusively on brachiopods (Biofacies 1). This is dominated by the *Lycophoria* and *Gonambonites* associations²⁶. Biofacies 2 is characterized by the trilobite genus *Asaphus* and, in the Kundan interval, also the brachiopods *Orthis* and *Orthambonites*. An intermediate biofacies dominated by the trilobite genera *Ptychopyge* (s.l.) and *Rhinoferus*, constitutes Biofacies 3. It is succeeded basin-wards by Biofacies 4, which is dominated by the trilobites *Megistaspis* and *Niobella*. Finally, the most offshore faunal association, which is here termed Biofacies 5, is dominated by the trilobites *Megalaspides* and *Paramegistaspis*.

Results

We present scaled 3rd and 4th order sea level curves through the succession (Fig. 4; Supp. Figs 1 and 2). These are based on detailed regional bio- and lithofacies changes through the studied time interval. The biofacies outline several major sea level oscillations, during an overall regressive trend through the early Mid Ordovician^{26,33}, including the onset of the GOBE in the early Darriwilian²¹. This regressive trend is recognized globally¹⁸.

Palaeoenvironmental changes based on biofacies. The upper Floian part of the succession (*Megistaspis estonica* trilobite Zone, See Supp. Fig. S1) is exclusively characterized by the deep water Biofacies 5. This level corresponds to the already falling sea level, terminating the *evae* highstand³⁴ and which ended in a transient lowstand at the Floian–Dapingian boundary. The succeeding lower part of the Dapingian Stage is dominated by Biofacies 4 and thus represents slightly shallower water conditions. Especially in the lower part of the Volkhov Regional Stage, in the *Asaphus broeggeri* Zone, the sea level fluctuated considerably, as witnessed by recurring shifts between Biofacies 4 and 2. In the upper part of the Volkhov Stage, the sea level was more stable, as signalled by a long interval characterized by Biofacies 3.

The lowermost Darriwilian (uppermost Volkhovian *Asaphus lepidurus* trilobite Zone) represents a prominent, long-lasting sea level drop characterized by Biofacies 2 (see Figs S1 and S2). In the succeeding Kunda Regional Stage, the lowermost biozone, the *Asaphus expansus* trilobite Zone, is much expanded in the Lynna River valley section, compared to that seen in Putilovo Quarry (compare the thickness of the biozones in Figs S1 and S2).

The *A. expansus* Zone commenced with *Orthis* dominated faunas, representing a small initial drowning, but still within the Biofacies 2 depth range. In the lower half of the *A. expansus* Zone this facies continues to dominate, although *Lycophoria* and *Gonambonites* dominated faunas become increasingly abundant upwards. These represent Biofacies 1 and signal an overall shallowing. The upper part of the *A. expansus* Zone and the lower part of the overlying *Asaphus raniceps* trilobite Zone is dominated by genera associated with Biofacies 1, thus signalling a major shallowing. These trends can also be recognized in Scania–Bornholm, Västergötland and the Oslo Region^{33,35} and this level is inferred to represent the second shallowest interval in the entire succession. It corresponds to the ‘Täljsten’ marker bed interval found in other areas of Baltoscandia³⁶, but can also be tracked globally²⁶.

Hereafter followed a substantial drowning, represented by the first influx of *Orthambonites* dominated faunas, which here is regarded as representing Biofacies 2. This corresponds to the Basal Llanvirn Drowning Event which is a globally recognized sea level rise³⁴. Most of the remaining part of the *A. raniceps* - *A. striatus* Zone is dominated by the *Orthambonites* association, i.e. Biofacies 2. However, the topmost beds record a significant shallowing which we regard as the shallowest interval in the studied succession, nearly completely dominated by fragmented, thick *Lycophoria* shells. It is possible that a full regression took place in the area at this level. This regression is also recorded globally¹⁸. Finally, the *Asaphus minor* trilobite Zone represents a more mixed biofacies, overall suggestive of deepening conditions.

Scaling the sea level curve. We have combined our sea level curve with existing Baltoscandian data^{26,33,34} in order to estimate the scale of the 3rd and 4th order sea level changes through the Early–Mid Ordovician (Floian–Darriwilian). The new scaled curve is based not only on the very detailed palaeoecological studies outlined above, but also on sections through offshore facies in Scania–Bornholm, intermediate facies in the Oslo Region and near-shore facies from other localities in Russia–Estonia^{26–28,33,34,37}. The fact that the sections constitute a depth transect on the palaeoshelf has guided scaling of the curve, as reconstructed sea level oscillations should satisfy observed changes both in deep and shallow settings. It appears that the cool water limestone facies started to develop well below the storm wave base; the lime mud deposited in the deeper part of the shelf is assumed to have been winnowed from the shallower shelf. The main clastic supply was from the west²⁰. The major sea level fall that took place in the early Mid Ordovician led to a westwards (downslope) migration of the limestone facies into deeper parts of the shelf that through most of the Ordovician was characterized by deposition of graptolite shale facies. This limestone tongue is named the Komstad Limestone in southernmost Scandinavia and the Huk Formation in southern Norway. As the sea level continued to fall, this limestone spread farther and farther west^{33,34,38}. Maximum western extent is seen in the upper part of the *A. raniceps* Zone, believed to signal peak lowstand. On the inner shelf most intervals with falling sea level and all lowstands were associated with cessation of deposition but it is uncertain whether the studied Russian and Estonian sections experienced a full regression during the most major lowstand peaks. Unambiguous sedimentological evidence of subaerial exposure is lacking, but the area was probably

close to or emergent during the late *A. raniceps* trilobite Zone. Overall, we estimate the sea level oscillations in the studied interval to be in the order of 150 m in Baltica. In comparison, global data suggest sea level fluctuations at least in the order of 80–90 m¹⁸, mirroring the trends in the 3rd order curve produced in this study (See Fig. 4).

Floian–Darriwilian $\delta^{18}\text{O}$ fluctuations in the successions. With respect to the geochemical data, the lower part of the succession commences with heavier brachiopod $\delta^{18}\text{O}$ values reflecting the intermediate palaeogeographical latitude of Baltica during the Floian (Fig. 4). In the uppermost Floian the values become more than 0.5‰ lighter ranging down to −6.0‰. The light oxygen isotope values continue during the Dapingian with baseline values fluctuating around −5.5‰. This trend is suddenly interrupted by a significant increase of more than 1‰ at the Dapingian–Darriwilian transition. The Kundan Stage continues this dramatic increase in $\delta^{18}\text{O}$ values with one sample even as high as −4.2‰ in the lowermost *A. raniceps* Zone. This is succeeded by a fast drop down to −5.4‰ before it rapidly increases to −4.7‰. The remaining part of the *A. raniceps* Zone exhibits decreasing $\delta^{18}\text{O}$ values although the topmost beds show dramatic increases up to −4.3‰. The uppermost biozone, the *A. minor* Zone, shows fluctuating values between −5.3‰ to −4.7‰.

Floian–Darriwilian $\delta^{13}\text{C}_{\text{carb}}$ correlation and the nature of the MDICE spike. The brachiopod $\delta^{13}\text{C}_{\text{carb}}$ values increase from below −2.4‰ to around 0.0‰ in the Billingen interval. The pronounced lighter $\delta^{13}\text{C}$ values in the lowermost beds probably correlate with the globally occurring negative excursion in the *Tetragraptus approximatus* graptolite Zone²². Hereafter follows a relatively stable interval with baseline values around −0.3‰ up through the first two biozones in the Volkhov Stage. This is succeeded by a slight decrease in baseline values in the uppermost Volkhovian *A. lepidurus* Zone. This decrease is continued into the lowermost Kundan before a sharp increase to positive values sets in in the uppermost *A. expansus* – lower *A. raniceps* zones. The more expanded Lynna section indicates a two-phased increase in the *A. expansus* interval (Fig. S2). Succeeding the peak in the lower *A. raniceps* Zone a rapid drop back to negative values (−0.7‰) follows. This is followed by a steady, continued increase up through the remaining part of the section with a peak around 0.7‰. This positive $\delta^{13}\text{C}$ trend towards the top of the succession clearly corresponds to the initial part of the globally occurring Middle Darriwilian Isotopic Carbon Excursion (MDICE)^{22,39}. This has previously been indirectly related to glaciation⁴⁰. Here we show, however, that the marked cooling started several million years prior to the main spike in the MDICE (not covered by the present study). We propose that this increase in the $\delta^{13}\text{C}_{\text{carb}}$ values in the lower Darriwilian was generated by an increase in bioproductivity caused by the rapidly accelerating radiation. Thus, the MDICE is the global response to the ignition of the GOBE.

Discussion

Apart from the decoupling of the sea level curve and the oxygen isotope ratios in the lowermost beds studied (Bilingen interval), the palaeoecologically derived 3rd and 4th order sea level curves and the $\delta^{18}\text{O}$ curves mirror each other throughout the studied interval; that is, heavier $\delta^{18}\text{O}$ values track falling sea level almost on a bed to bed scale. In the uppermost Billingen interval a short warming event has been demonstrated by the influx of tropical conodonts into Baltica⁴¹. This warming event is captured by the $\delta^{18}\text{O}$ isotopes showing a rapid drop of more than 0.5‰. This suggests that the heavier $\delta^{18}\text{O}$ values below indicate that Baltica was positioned at sufficiently high southerly latitudes to generate such high $\delta^{18}\text{O}$ values. As for the peak lowstand interval in the Kundan *A. expansus*–*A. raniceps* interval, this correlates with the highest values in the $\delta^{18}\text{O}$ curve.

This sudden shift to heavier, strongly fluctuating $\delta^{18}\text{O}$ values just after the Dapingian–Darriwilian boundary with 1 to 1.5‰ shifts in the Kundan interval are remarkably similar to the $\delta^{18}\text{O}$ pattern observed during the Quaternary^{42,43}. Accepting that no major salinity changes took place in this well ventilated, mid-latitude palaeo-basin, this oxygen isotope increase is suggestive of a 4 to 5 °C cooling⁴⁴. The counterclockwise rotation of Baltica¹⁷ at this time could theoretically have contributed to this shift as the ocean gateway turns increasingly towards the south, theoretically permitting cooler ocean currents onto the platform (Fig. 4). However, in that case, a more gradual shift to heavier oxygen isotopes would be expected. Further, the palaeoecological proxies indeed support a pronounced sea level fall controlled by glacioeustasy as witnessed by the rapid shifts in biofacies (Supp. Figs 1 and 2). An overall 4–5 °C decrease across the Dapingian–Darriwilian transition, indicated by data from benthic fossils, thus probably represents a temperature shift at the sea floor (see discussion of assumptions in the Supplementary Information file). This is a conservative estimate because Baltica drifted more than 1,000 km closer to the Equator through the studied interval¹⁷. This continued northward drift towards warmer, mid-latitude climate belts, ought to some extent have counter-acted the cooling climate. However, our two separate proxies suggest an opposing climate signal. Similarly, because of the regression trend we would expect warmer water across the craton, but the opposite is true. We conclude that the observed fall in sea bed temperature represents a major ocean cooling event and a shift from greenhouse to icehouse causing a major glacioeustatic sea level drop. We estimate the sea level fall to have been at least 150 m from the global upper Floian *evae* highstand^{18,34} to the most shallow water facies in the uppermost *raniceps* Zone in the lower Darriwilian. This is in the same order of magnitude as estimates for the Pleistocene sea level fluctuations⁴⁵. We argue that only glacioeustatic oscillations could have enabled the large sea level drop through the studied succession. The cooling and rapidly fluctuating sea level reflects the waxing and waning of ice caps at the palaeo South Pole. Thus, we suggest an onset of Ordovician icehouse conditions which commenced around the Lower/Middle Ordovician boundary, significantly changing the traditional view of the Ordovician as a sustained greenhouse interval.

What caused this sudden cooling is not resolved by the current study. Previously suggested drivers for the general cooling climate trend in the Ordovician^{6,11} are mostly based on gradual processes, such as continental arc collisions¹⁴ or the colonisation of land plants¹¹. These are drivers that are primarily inferred from a record of reduced weathering, as witnessed by the declining ⁸⁷Sr/⁸⁶Sr record through the Ordovician²³. This, again, is interpreted to

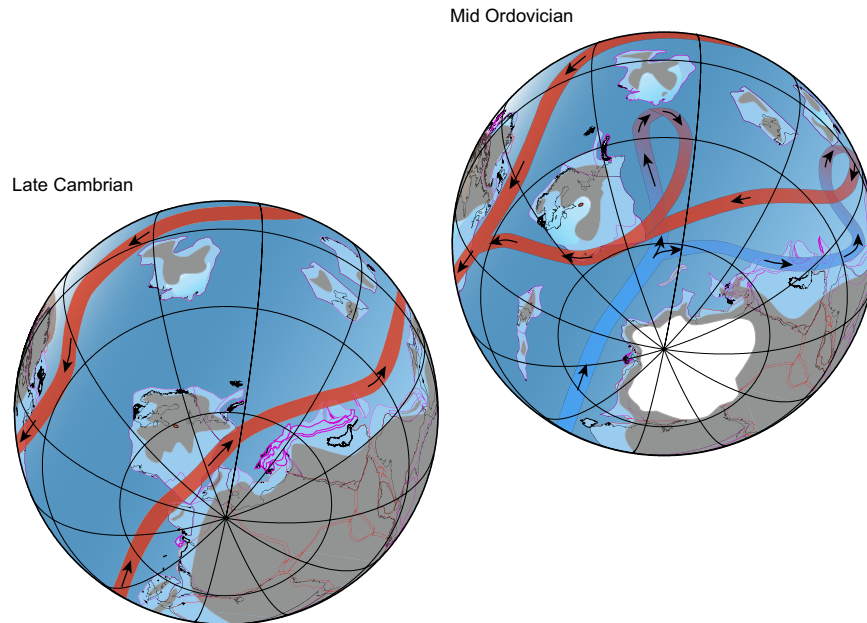


Figure 5. Simplified hypothetical ocean conveyor belt circulation scenarios for the late Cambrian and Mid Ordovician worlds. During the late Cambrian greenhouse, latitudinal temperature gradients were weak resulting in warm surface water circulation, but lacked movement of deep-water masses. This resulted in widespread euxinia at the sea floor. The onset of icehouse conditions during the Mid Ordovician intensified the latitudinal and bathymetrical temperature and oxygen gradients. This initiated the formation of deep ocean circulation and thus the Great Ocean Conveyor Belt. Ocean currents are based on the literature^{49–55}, but inferred based on the circulation pattern of the present day Great Ocean Conveyor Belt. Palaeogeographic projection provided by Trond Torsvik, Norwegian Geological Survey, based on the software package BugPlates⁵⁷: <http://www.geodynamics.no/Web/Content/Software/>.

reflect a slow decline of CO₂ levels. This scenario is incompatible with the current study as these drivers probably did not contribute to the sudden shift in climate demonstrated by the present study.

The sudden initiation of icehouse conditions during the Mid Ordovician thus represents a paradigm shift in the way we view Ordovician climate. The onset of the greatest radiation event of the Phanerozoic may now be addressed against a background of a sudden shift in climate. This would have had a profound impact as cooler ocean currents increased thermohaline circulation in the oceans, creating upwelling zones where plankton evolved and radiated. Moreover, oxygen was more accessible for organisms, once ocean temperatures fell, as predicted by Henry's Law.

The onset of the Mid Ordovician icehouse marked a dramatic climatic change, contrasting conditions in the late Cambrian world. This clearly had a fundamental impact on ocean circulation patterns (Fig. 5). Widespread black shales suggest that anoxia was prevalent on late Cambrian ocean floors and that water circulation was at best sluggish^{46,47}. During the Ordovician, the increased latitudinal temperature gradients, as well as those for bathymetrical oxygen, encouraged by icehouse conditions initiated thermohaline circulation bringing nutrient rich, cold bottom waters to the surface. This effect was further intensified by a drastically rising sea level, which flooded the continents, creating epicontinental seas that were shallow and thus more easily heated. In addition, the continued northbound drift of several continents and microcontinents towards lower latitudes further intensified the thermohaline circulation through the Ordovician as more and more shelf areas impinged on lower latitudes transporting larger areas with upwelling zones into tropical regions.

We speculate, therefore, that the initiation of a Lower Palaeozoic Great Ocean Conveyor Belt encouraged the GOBE by creating new viable ecospace in the form of nutrient rich upwelling zones. This initiated a revolution not only for the primary producers, but for the entire trophic chain.

Methods

Our dataset consists of ~30,000 brachiopods and 15,000 trilobites collected bed-by-bed from several localities in the eastern Baltic–western Russian region along a 400 km transect. All specimens were prepared mechanically using air chisels and registered in a database. Specimens were identified at the lowest possible taxonomical level. Sections were correlated using bio- and lithostratigraphy, as well as ecostratigraphy for the upper Volkhovian–Kundan interval²⁶. For the current study, an estimate of the absolute sea level changes through the studied interval were conducted based on compilation of regional sedimentological and palaeontological data. The presented stable isotope data originate from two of these sections, which are located 80 km apart in western Russia. Calcite for stable isotope analysis was carefully extracted from the secondary layer of the brachiopod shells, as this part of the brachiopod shell is most likely to carry intact geochemical information (see Supplementary Information). One shell was selected from each bed in the two studied sections. Up to three samples were taken from each shell if possible. In one specimen seven samples were taken to study the expected seasonal variation. Thus, in all,

the dataset comprises 385 samples obtained from 234 shells. To avoid using material that had been subjected to secondary diagenetic overprint, all samples were photographed under SEM to visually screen for ultrastructure signs of diagenetic alteration. Further, trace element analyses were conducted to study Mn/Ca, Mg/Ca and Sr/Ca ratios in order to assess the preservational state of the shells analyzed. Here a limit of 250 µg/g (=0.455 mmolMn per mol Ca) was applied for Mn to indicate good preservation⁴⁸.

References

1. Sepkoski, Jr. J. A factor analytic description of the Phanerozoic marine fossil record. *Paleobiology* **7**, 36–53 (1981).
2. Sepkoski, Jr. J. A compendium of fossil marine animal genera. *B. Amer. Pal.* **363**, 1–560 (2002).
3. Alroy, J. *et al.* Phanerozoic trends in the global diversity of marine invertebrates. *Science* **321**, 97–100 (2008).
4. Alroy, J. *et al.* The shifting balance of diversity among major marine animal groups. *Science* **329**, 1191–1194 (2010).
5. Rohde, R. A. & Muller, R. A. Cycles in fossil diversity. *Nature* **434**, 208–210 (2005).
6. Trotter, J. A., Williams, I. S., Barnes, C. R., Lécuyer, C. & Nicoll, R. S. Did cooling oceans trigger Ordovician biodiversification? Evidence from conodonts thermometry. *Science* **321**, 550–554 (2008).
7. Harper, D. A. T. The Ordovician biodiversification: Setting an agenda for marine life. *Palaeogeogr. Palaeoclimatol. Palaeoecol.* **232**, 148–166 (2006).
8. Cooper, R. A., Sadler, P. M., Munnecke, A. & Crampton, J. S. Graptoloid evolutionary rates track Ordovician–Silurian global climate change. *Geol. Mag.* **151**, 349–364 (2014).
9. Harper, D. A. T. *et al.* Biodiversity, biogeography and phylogeography of Ordovician rhynchonelliform brachiopods. *Mem. Geol. Soc. London* **38**, 127–144 (2013).
10. Servais, T. *et al.* The onset of the ‘Ordovician Plankton Revolution’ in the late Cambrian. *Palaeogeogr. Palaeoclimatol. Palaeoecol.* (in press). doi:10.1016/j.palaeo.2015.11.003
11. Lenton, T. M., Crouch, M., Johnson, M., Pires, N. & Dolan, L. First plants cooled the Ordovician. *Nat. Geosci.* **5**, 86–89 (2012).
12. Schmitz, B. *et al.* Asteroid breakup linked to the Great Ordovician Biodiversification Event. *Nat. Geosci.* **1**, 49–53 (2008).
13. Munnecke, A. & Servais, T. What caused the Ordovician biodiversification? *Palaeogeogr. Palaeoclimatol. Palaeoecol.* **245**, 1–4 (2007).
14. McKenzie, N. R., Hughes, N. C., Gill, B. C. & Myrow, P. M. Plate tectonic influences on Neoproterozoic–early Paleozoic climate and animal evolution. *Geology*, doi: 10.1130/G34962.1 (2014).
15. Servais, T. *et al.* The Ordovician Biodiversification: revolution in the oceanic trophic chain. *Lethaia* **41**, 99–109 (2008).
16. Wheeley, J. R., Smith, M. P. & Boomer, I. Oxygen isotope variability in conodonts: implications for reconstructing Palaeozoic palaeoclimates and palaeoceanography. *J. Geol. Soc. London* **169**, 239–250 (2012).
17. Torsvik, T. H. *et al.* Phanerozoic polar wander, palaeogeography and dynamics. *Earth-Sci. Rev.* **114**, 325–368 (2012).
18. Haq, B. U. & Shutter, S. R. A chronology of Paleozoic sea-level changes. *Science* **322**, 64–68 (2008).
19. Hallam, A. *Phanerozoic sea-level changes* (Columbia University Press, 1992).
20. Jaanusson, V. Aspects of carbonate sedimentation in the Ordovician of Baltoscandia. *Lethaia* **6**, 11–34 (1973).
21. Rasmussen, C. M. Ø., Hansen, J. & Harper, D. A. T. Baltica: A mid Ordovician diversity hotspot. *Hist. Biol.* **19**, 255–261 (2007).
22. Bergström, S. M., Chen, X., Gutiérrez-Marco, J. C. & Dronov, A. The new chronostratigraphic classification of the Ordovician System and its relations to major regional series and stages and to $\delta^{13}\text{C}$ chemostratigraphy. *Lethaia* **42**, 97–107 (2009).
23. McArthur, J. M., Howarth, R. J. & Shields, G. A. In *The Geologic Time Scale* (eds Gradstein, F. M. *et al.*) Ch. 7, 127–144 (Elsevier, 2012).
24. Pärnaste, H., Bergström, J. & Zhiyi, Z. High resolution trilobite stratigraphy of the Lower-Middle Ordovician Öland Series of Baltoscandia. *Geol. Mag.* **150**, 509–518 (2013).
25. Cooper, R. A., Sadler, P. M., Hammer, O., & Gradstein, F. M. In *The Geologic Time Scale* (eds Gradstein, F. M. *et al.*) Ch. 20, 489–523 (Elsevier, 2012).
26. Rasmussen, C. M. Ø., Nielsen, A. T. & Harper, D. A. T. Ecostratigraphical interpretation of lower Middle Ordovician East Baltic sections based on brachiopods. *Geol. Mag.* **146**, 717–731 (2009).
27. Hansen, J. & Harper, D. A. T. Brachiopod macrofaunal distribution through the upper Volkhov – lower Kunda (Lower Ordovician) rocks, Lynna River, St. Petersburg region. *B. Geol. Soc. Denmark* **50**, 45–55 (2003).
28. Hansen, T. & Nielsen, A. T. Upper Arenig trilobite biostratigraphy and sea-level changes at Lynna River near Volkhov, Russia. *B. Geol. Soc. Denmark* **50**, 105–114 (2003).
29. Rasmussen, C. M. Ø. & Harper, D. A. T. Resolving early Mid Ordovician (Kundan) bioevents in the East Baltic based on brachiopods. *Geobios* **41**, 533–542 (2008).
30. Egerquist, E. Early Ordovician (Billingen–Volkhov stages) Brachiopod faunas from the NW Russia. *Acta Univ. Carol. – Geol.* **43**, 341–343 (1999).
31. Jakobsen, K. G. Lower-Middle Ordovician at Putilovo, St. Petersburg region, Russia: biozonation and palaeoecology based on trilobites [in Danish] Cand. Scient. thesis, University of Copenhagen, (2005).
32. Hammer, Ø. & Harper, D. A. T. *Palaeontological Data Analysis*. 1st edn, (Blackwell Publishing, 2006).
33. Nielsen, A. T. Trilobite systematics, biostratigraphy and palaeoecology of the Lower Ordovician Komstad Limestone and Huk Formations, Southern Scandinavia. *Fossils Strata* **38**, 1–374 (1995).
34. Nielsen, A. T. In *The Great Ordovician Biodiversification Event* (eds Webby, B. D. *et al.*) Ch. 10, 84–93 (Columbia University Press, 2004).
35. Lindskog, A., Eriksson, M. E. & Pettersson, A. M. L. The Volkhov–Kunda transition and the base of the Hølen Limestone at Kinnekulle, Västergötland, Sweden. *GFF* **136**, 167–171 (2014).
36. Eriksson, M. E. *et al.* Biotic dynamics and carbonate microfacies of the conspicuous Darriwilian (Middle Ordovician) ‘Täljsten’ interval, south-central Sweden. *Palaeogeogr. Palaeoclimatol. Palaeoecol.* **367–368**, 89–103 (2012).
37. Villumsen, J. The trilobite zonation at the Volkhov/Kunda boundary, lower Middle Ordovician in Hällekis Quarry, Västergötland, Sweden [in Danish] Cand. Scient. thesis, University of Copenhagen, (2001).
38. Männil, R. *Evolution of the Baltic Basin during the Ordovician*. (Valgus Publishers, 1966).
39. Schmitz, B., Bergström, S. M. & Xiaofeng, W. The middle Darriwilian (Ordovician) ^{13}C excursion (MDICE) discovered in the Yangtze Platform succession in China: implications of its first recorded occurrences outside Baltoscandia. *J. Geol. Soc. London* **167**, 249–259 (2010).
40. Chens, L. *et al.* Long-period orbital climate forcing in the early Palaeozoic? *J. Geol. Soc. London* **170**, 707–710 (2013).
41. Bagnoli, G. & Stouge, S. Lower Ordovician (Billingenian–Kunda) conodont zonation and provinces based on sections from Horns Udde, north Öland, Sweden. *B. Soc. Pal. Italiana* **35**, 109–163 (1997).
42. Raymo, M. E. The initiation of the northern hemisphere glaciation. *Annu. Rev. Earth Planet. Sci.* **22**, 353–383 (1994).
43. Lisiecki, L. E. & Raymo, M. E. A Pliocene–Pleistocene stack of 57 globally distributed benthic $\delta^{18}\text{O}$ records. *Paleoceanography* **20**, 1–17.
44. O’Neil, J. R., Clayton, R. N. & Mayeda, T. K. Oxygen isotope fractionation in divalent metal carbonates. *J. Chem. Phys.* **51**, 5547–5558 (1969).

45. Bintanja, R., van de Wal, R. S. W. & Oerlemans, J. Modelled atmospheric temperatures and global sea levels over the past million years. *Nature* **437**, 125–128.
46. Gill, B. G. *et al.* Geochemical evidence for widespread euxinia in the Later Cambrian ocean. *Nature* **469**, 80–83 (2011).
47. Berry, W. B. N. & Wilde, P. Progressive ventilation of the oceans; an explanation for the distribution of the lower Paleozoic black shales. *Am. J. Sci.* **278**, 257–275 (1978).
48. Korte, C., Jones, P. J., Brand, U., Mertmann, D. & Veizer, J. Oxygen isotope values from high-latitudes: Clues for Permian sea-surface temperature gradients and Late Palaeozoic deglaciation. *Palaeogeogr. Palaeoclimatol. Palaeoecol.* **269**, 1–16, doi: 10.1016/j.palaeo.2008.06.012. (2008).
49. Cocks, L. R. M. & Torsvik, T. H. Siberia, the wandering northern terrane, and its changing geography through the Palaeozoic. *Earth-Sci. Rev.* **82**, 29–74 (2007).
50. Torsvik, T. H. & Cocks, L. R. M. In Early Palaeozoic Peri-Gondwana Terranes: new insights from tectonics and biogeography. *Geological Society, London, Special Publications*, **325**, (ed M.G., Bassett) Ch 1, 3–21 (The Geological Society of London, 2009).
51. Christiansen, J. L. & Stouge, S. Oceanic circulation as an element in palaeogeographical reconstructions: the Arenig (early Ordovician) as an example. *Terra Nova* **11**, 73–78 (1999).
52. Wilde, P. In *Advances in Ordovician Geology* Paper 5 90–9 (eds Barnes, C. F. & Williams, S. H.), 283–298 (Geological Survey of Canada, 1991).
53. Herrmann, A. D., Haupt, B. J., Patzkowsky, M. E., Seidov, D. & Slingerland, R. L. Response of Late Ordovician paleoceanography to changes in sea level, continental drift, and atmospheric pCO₂: potential causes for long-term cooling and glaciation. *Palaeogeogr. Palaeoclimatol. Palaeoecol.* **210**, 385–401 (2004).
54. Poussart, P. F., Weaver, A. J. & Barnes, C. R. Late Ordovician glaciation under high atmospheric CO₂: a coupled model analysis. *Paleoceanography* **14**, 542–558 (1999).
55. Servais, T., Danelian, T., Harper, D. A. T. & Munnecke, A. Possible oceanic circulation patterns, surface water currents and upwelling zones in the Early Palaeozoic. *GFF* **136**, 229–233 (2014).
56. Hints, L. & Harper, D. A. T. Review of the Ordovician rhynchonelliformean Brachiopoda of the East Baltic: their distribution and biofacies. *B. Geol. Soc. Denmark* **50**, 29–43 (2003).
57. BugPlates Team. BugPlates: Linking biogeography and palaeogeography. Centre for Geodynamics, Trondheim, Norway. URL: <http://www.geodynamics.com> (2009).

Acknowledgements

Our expeditions to Russia were mainly funded by the Carlsberg Foundation. C.M.Ø.R. and D.A.T.H. are particularly grateful to the Danish Council for Independent Research | Natural Sciences for their support of this specific project. C.M.Ø.R. further acknowledge support from the VILLUM Foundations Young Investigator Programme. A.L. was funded by the Royal Swedish Physiographic Society in Lund. M.E.E. and A.L. thank Birger Schmitz, Lund, for facilitating the 2012 Russia field trip. All material is deposited in the Natural History Museum of Denmark.

Author Contributions

C.M.Ø.R., C.V.U., C.K., A.T.N. and D.A.T.H. designed the research. C.M.Ø.R., K.G.J., J.H., T.H., A.D., A.T.N. and D.A.T.H. conducted the field work and performed the taxonomical and palaeoecological analysis. The Sea level curves were constructed by A.T.N., C.M.Ø.R., K.G.J., A.D., M.E.E. and A.L.; C.M.Ø.R., C.V.U., C.K. and R.F. performed the geochemical analysis. A.D. constructed the type logs. A.D., A.L. and M.E.E. contributed with sedimentological input. D.A.T.H. and A.T.N. secured funding for the main fieldwork. C.M.Ø.R., A.T.N., C.V.U. and D.A.T.H. wrote the paper, with contributions from all authors.

Additional Information

Supplementary information accompanies this paper at <http://www.nature.com/srep>

Competing financial interests: The authors declare no competing financial interests.

How to cite this article: Rasmussen, C. M. Ø. *et al.* Onset of main Phanerozoic marine radiation sparked by emerging Mid Ordovician icehouse. *Sci. Rep.* **6**, 18884; doi: 10.1038/srep18884 (2016).



This work is licensed under a Creative Commons Attribution 4.0 International License. The images or other third party material in this article are included in the article's Creative Commons license, unless indicated otherwise in the credit line; if the material is not included under the Creative Commons license, users will need to obtain permission from the license holder to reproduce the material. To view a copy of this license, visit <http://creativecommons.org/licenses/by/4.0/>